THE MESSENGER

EL MENSAJERO

Paranal
La Silla
La Serena
Santiago
Munich

No. 95 – March 1999

TELESCOPES AND INSTRUMENTATION

ISAAC at the VLT

A. MOORWOOD, J.-G. CUBY, P. BALLESTER, P. BIEREICHEL, J. BRYNNEL, R. CONZELMANN, B. DELABRE, N. DEVILLARD, A. VAN DIJSSELDONK, G. FINGER, H. GEMPERLEIN, C. LIDMAN, T. HERLIN, G. HUSTER, J. KNUDSTRUP, J.-L. LIZON, H. MEHRGAN, M. MEYER, G. NICOLINI, A. SILBER, J. SPYROMILIO, J. STEGMEIER

ESO

1. Introduction

ISAAC (Infrared Spectrometer and Array Camera) provides for 1–5 µm imaging; 1–2.5 µm polarimetry and 1–5 µm spectroscopy and is the first VLT instrument fully developed by ESO. Figure1 shows it mounted on the adapter/rotator at the Nasmyth B focus of the first of the four 8.2-m VLT Unit Telescopes. ISAAC itself is cryogenically cooled and housed within a 1.6-m diameter vacuum vessel enclosed by the red protective cover seen in this photograph. The large unit to the right, flanked by the two racks of control electronics, is the cable co-rotator system which carries the electrical cables and closed-cycle cooler hoses to the instrument and rotates with it as the telescope tracks objects on the sky. Following integration and extensive testing in Garching, ISAAC was delivered to the Paranal Observatory in June 1998 where it was re-assembled and re-tested in the Integration Laboratory prior to installation on the telescope, as scheduled, on November 14th. First light images were already shown in *The Messenger* 94, 7, and accompanied by a very short article written in the VLT control room while the

Figure 1: ISAAC installed at the Nasmyth B focus of the VLT UT1. The instrument, enclosed in its protective red cover, is attached to the adapter/rotator system at the left and has a total weight of around 1.5 tons. The box at the left contains some of the electronics required for controlling and reading the two infrared array detectors. To the right is the co-rotator system that transfers all the electrical cables and gas hoses for the closed-cycle coolers to the instrument and rotates with it and the adapter. At each side of the co-rotator are cabinets containing electronics for controlling and monitoring the instrument functions and the vacuum and cryogenic system. At the bottom can be seen part of the platform to which the instrument is attached for installation, removal and maintenance activities.

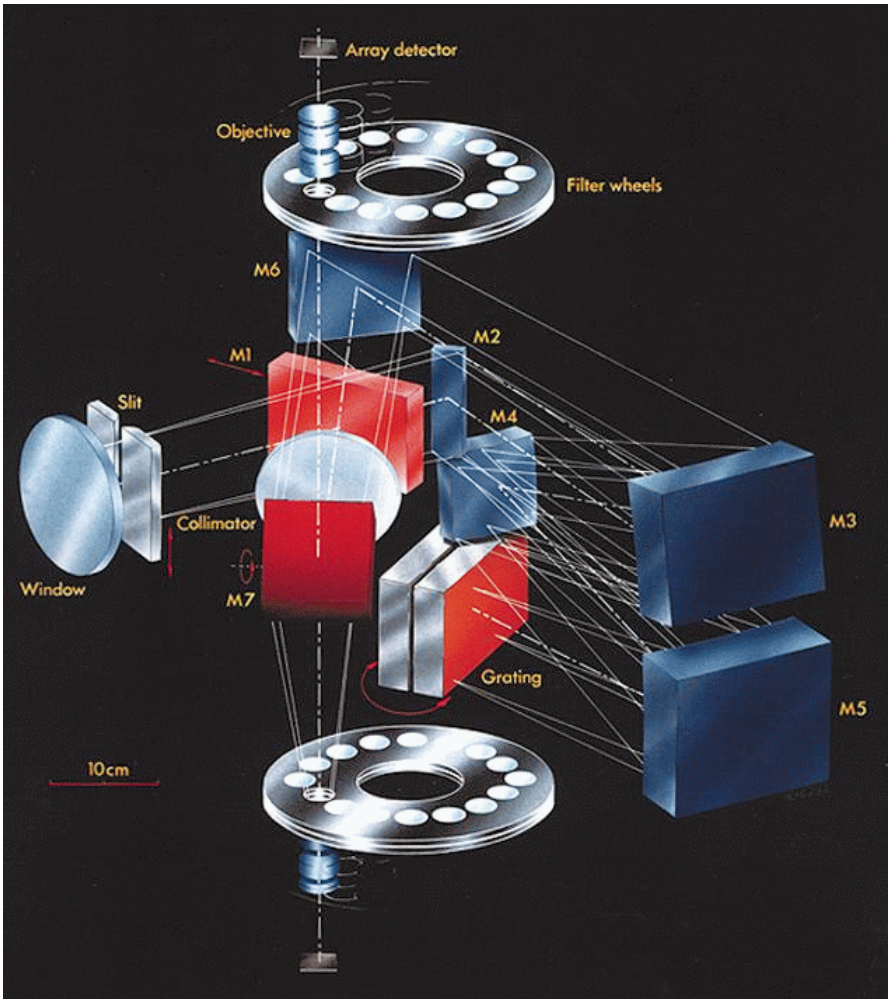

Figure 2: Optical layout of ISAAC. See text for a detailed explanation.

first tests were still in progress. Just prior to the planned start of routine operations on April 1st, it is appropriate here to briefly recall its design and development, report on its performance during the commissioning tests and present some spectra of relatively faint objects which illustrate further the new scientific capabilities now offered by this instrument.

2. Scientific Capabilities

Scientific interest in ISAAC encompasses most topics in modern astronomy from the study of faint outer solar-system bodies to the most distant galaxies and clusters. In these and other areas, such as the study of Brown Dwarfs and low-mass stars, its particular strength lies in the possibility of both making deep imaging observations and surveys and following them up spectroscopically. There is no space here to enter into a detailed discussion of the scientific results and discoveries to be expected. It is, however, interesting to recall that near-infrared imaging and spectroscopy of high redshift galaxies was highlighted in the original ISAAC Design and Implementation Plan of October 1991 as the area which could potentially gain most from such an instrument on a large telescope. More specific topics mentioned were the observation of 'visible' lines for redshift determinations, deep searches for extremely red, possibly primeval galaxies, studies of cluster evolution, etc. Although apparently trivial as a prophecy now, few high z galaxies were actually known at that time and the enormous level of current activity and interest in this area together with the relatively large fraction of ISAAC observing time allocated to it in P 63 is therefore rather comforting. That the required sensitivity can actually be reached is also supported by some of the spectra obtained during commissioning and shown here.

Figure 3: ISAAC with its front vacuum flange removed revealing the slit/mask wheel and the casting used to support its various opto-mechanical functions, including the two cameras which are partly visible to the upper and lower right of the centre.

3. Observational Modes

ISAAC offers the following observational modes:

- Imaging through broad- and narrow-band filters
  - 0.9–2.5 µm with a 2.5 × 2.5′ field of view and 0.147″ pixels
  - 2.5–5 µm with a 40 × 40″ max. field of view and pixels of 0.16″ and 0.08″
- Imaging polarimetry
  - 0.9–2.5 µm using a Wollaston prism with broad-band and a limited set of narrow-band filters
- Spectroscopy at Rs ∼ 500 and 3000 and slit widths of 0.3, 0.6, 1 and 2″
  - 0.9–2.5 µm with a slit length of 2′
  - 2.5–5 µm with a slit length of 40″

The more detailed information required for making an observing proposal can be found on the Web (http://www.eso.org/observing/observing.html).

4. Design and Development

Figure 2 shows the optical layout of ISAAC. It contains two cameras (each comprising 2 filter wheels, an objective wheel and an array detector) one of which is optimised for the 1–2.5 µm and the other for the 2.5–5 µm spectral ranges. For imaging and polarimetry the light entering the window at the left passes through the slit/mask wheel, is diverted by the mirror M1 through the 16-cm-diameter BaF2 collimator/field lens and to the required camera by the M7 selector mirror. For spectroscopy the mirror M1 is retracted, allowing light from the slit to

pass through the spectrometer unit to form an intermediate spectrum close to M6 which is then re-imaged by the selected camera. The spectrometer unit consists of 2 back-to-back mounted gratings – for the low- and medium-resolution modes – and a mirror system comprising three hyperbolic mirrors (M3, M4, M5), which were diamond turned on nickel-coated aluminium and then hand post polished and gold coated. This system is used both to collimate the 10-cm-diameter beam and to form the intermediate spectrum after dispersion at the grating. Attached to the front of the instrument is the pre-slit unit containing a pupil lens, integrating sphere, continuum plus line lamps for flat fielding and wavelength calibration and a technical CCD for slit viewing.

The 1–2.5 µm (SW) 'arm' is equipped with a 1024 × 1024 pixel Hg:Cd:Te array manufactured by the Rockwell International Science Center and the 2.5–5 µm 'arm' with a 256 × 256 InSb array from the Santa Barbara Research Center. Detector control and data acquisition is via the ESO-developed high-speed IRACE system (Meyer et al. 1996).

Most of the moving functions in ISAAC (slit/mask wheel, M1 and M7 selector mirrors, grating, filter and objective wheels) are mounted on paired, angular contact, bearings and driven by 5-phase stepper motors (modified at ESO for cryogenic operation) and stainless steel worm gears acting on Vespel or Nylcast toothed wheels attached to the functions. The linear lens collimator drive employs a preloaded roller screw. Initialisation of the functions is by means of magnetic sensors. In the case of the bearings, the steel balls were replaced by tungsten carbide ones and the separators by self-lubricating Nylcast cages impregnated with 321R from Dow Corning. Because of the inherent difficulty in developing such high-precision moving functions for operation at cryogenic temperatures in vacuum, both the individual components as well as a complete prototype unit were extensively tested before the Final Design Review of the instrument. The various optomechanical functions, including their drive systems, are all supported by a cast aluminium structure surrounded by a radiation shield and attached to the vacuum vessel by two fibreglass 'spiders'. Figure 3 shows ISAAC with the front cover of its vacuum vessel removed and provides a view of the cast structure plus the large slit/mask wheel and parts of the two cameras. Access to the spectrometer is by removing the rear vacuum flange. Total mass of the cryogenically cooled part is 350 kg. Despite this large mass, it can be cooled to its operating temperature of 70 K (and the detectors to as low as 25 K) in 24 hours using a liquid-nitrogen continuous-flow circuit during this phase to boost the cooling power of the two closed-cycle coolers used to maintain the required temperatures during normal operation. Evacuation is by means of a backing pump behind a turbomolecular pump flanged directly onto the vacuum vessel. All cryogenic operations during cool-down and warm-up are controlled automatically by the control system which also monitors temperatures/pressure and sounds safety alarms and/or initiates safety features (e.g. automatic warming up of the detectors in case of loss of cooling power or a rapid pressure rise). Additional details of the design have been given by Moorwood (1996) and of the integration phase in Garching by Lizon (1996).

Figure 4: Colour composite image of the merging galaxy system ESO202–G23 which combines a 1200s ISAAC H (1.65 µm) band exposure with B (1800s) and R (900s) images obtained with the VLT test camera. The field shown here is ∼1.5′ with north at the top and east to the left and the seeing was ∼ 0.4″. Visible are at least one Active Galaxy Nucleus with an associated ionisation cone; a blue star-forming complex to the south; and a complicated pattern of emission resulting from the merger and heavy extinction. Of additional interest is the arc of more distant red galaxies in the lower part of the image.

5. Performance

Based on the commissioning tests and observations made so far, the astronomical performance of ISAAC fully lives up to expectations. The combination of excellent telescope and instrument optical quality delivers fully seeing-limited images with a smallest FWHM so far of 0.28″. The arrays are cosmetically good, the fields 'clean' and flat (to a few per cent before flat fielding), internal flexure is less than 0.5 pixel and the limiting magnitudes are set by the sky + telescope background and the seeing. For observations in the thermal infrared, beyond 2.5 µm, the telescope passed with flying colours its most difficult challenge of performing the active optics corrections while nodding plus chopping and field stabilising with M2.

Given the new maturity of infrared capabilities, it is likely that many scientific programmes will increasingly combine visible and infrared data. As an example, Figure 4 shows a colour composite (B, R, H(1.65 µm)) image of the merging active galaxy system ESO 202-G23 made by combining images obtained with ISAAC and the VLT test camera and which adds to the diagnostic power of the visible or infrared images alone. A selection of other illustrative images has already been presented in *The Messenger* 94, 7 (1998) and on the Web (http://www.eso.org/outreach/press-rel).

Low-resolution spectroscopy at most wavelengths is also background limited by the radiation from the sky and tele-

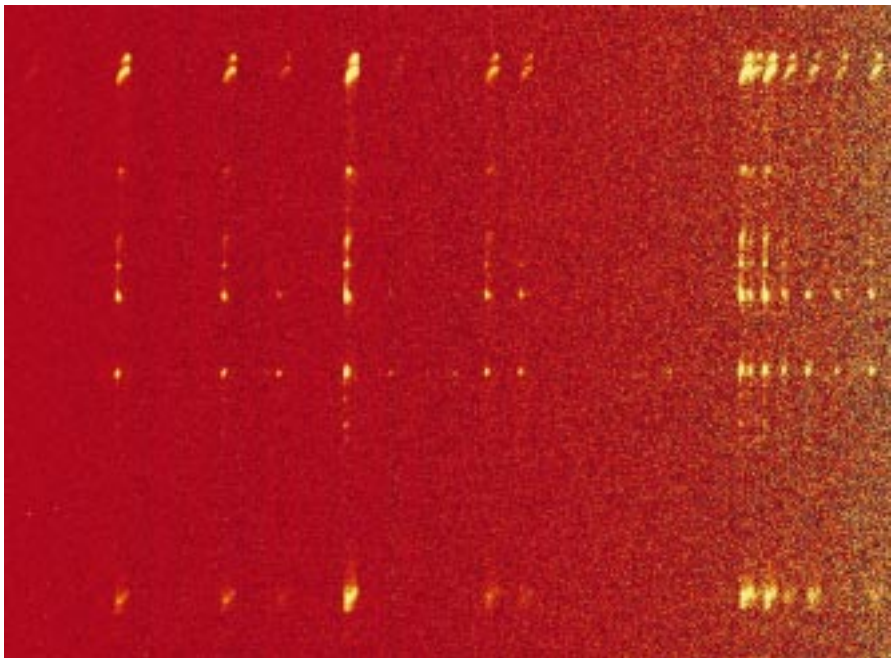

Figure 5: Low-resolution 2–2.5 µm spectral image of HH212 which fully exploits the 2′ long slit. This galactic object is believed to harbour a heavily obscured protostar that has expelled material periodically during it evolution. What is remarkable is the degree of symmetry of the 'bullets' ejected in opposite directions. Each of the 'images' seen here corresponds to a different emission line of interstellar molecular hydrogen that has been excited by the impact of the ejected material.

scope. Examples are shown in Figures 5 and 6 which show a K band spectral image of the fascinating Herbig Haro object HH212 and J, H, K band spectra of the radio galaxy MRC0406-244 plus two extremely red, nearby, galaxies. At medium resolution (R ~ 3000) in the J and H bands, however, regions between the OH sky lines open up where the background continuum has been measured to be extremely low (< 0.1 e^-/s). As the detector dark current is even lower than this, sensitivity in these regions is limited essentially by the detector read noise (< 10 e^-), bad pixels and cosmic rays. This is illustrated by Figure 7 which shows medium-resolution spectra around 1.06 µm of redshifted Hα (+[NII]) emission in two $z \sim 0.62$ galaxies from the CFRS catalogue which are only a few arcsec apart on the sky (Hammer et al. 1995). Finally, Figure 8 shows an example of medium-resolution 'imaging' spectroscopy in the form of a spectrum of SN 1987A obtained through the 2″ slit and with the grating set close to the He I 1.083 µm line.

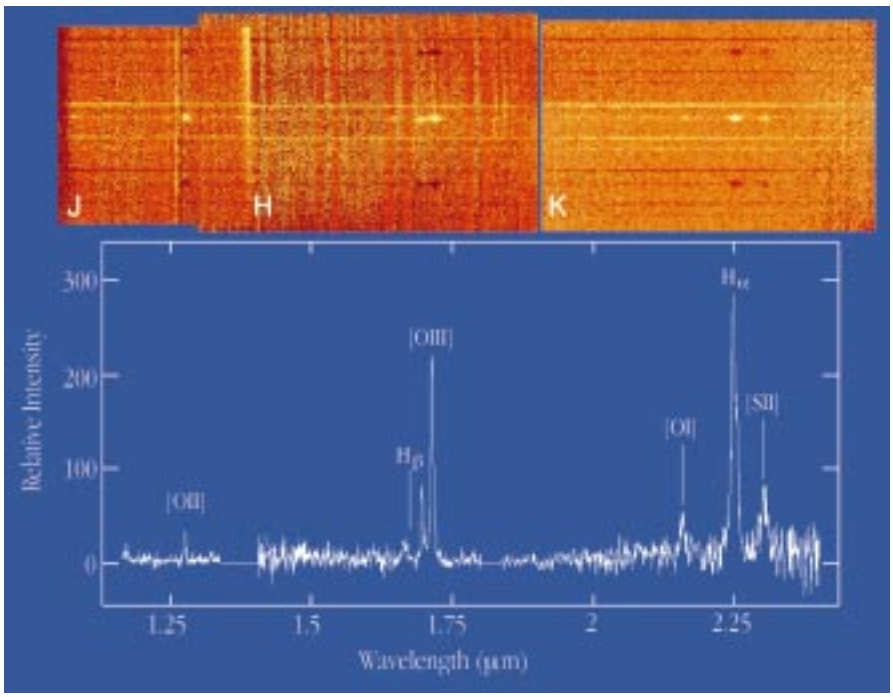

Figure 6: The upper panel shows a montage of low-resolution (R ~ 500) spectral images covering most of the 1–2.5 µm region of the z = 2.4 radio galaxy MRC0406–244 plus two extremely red (R-K > 5) galaxies below and an anonymous one above. Integration times were 2 hours in the J and 1 hour in H and K bands. The negative images of the spectra result from the technique used for sky subtraction, and the vertical stripes are due to increased photon shot noise at the positions of OH night sky lines. The extracted spectrum of the radio galaxy in the lower panel shows the prominent, redshifted, emission lines [OII], Hβ [OIII] (doublet), [OI], Hα and [SII] (doublet) normally observed at visible wavelengths in nearby objects. The apparent absence of these lines in the spectra of the companion red galaxies casts some doubt on the suggested possibility that they are members of a cluster at the same redshift as the radio galaxy.

Because performance is a strong function of mode, wavelength, conditions, etc, it is difficult, and potentially misleading, to summarise it in a few numbers here. The information is available, however, and has been incorporated into the ISAAC Exposure Time Calculators, the ISAAC Users Manual and other information which is available and will be maintained on the Web (http://www.eso.org/observing/observing.html).

6. Observing with ISAAC

Routine observations with ISAAC are planned to start in P 63 on April 1st, 1999. Of course, ISAAC is fully embedded in the VLT operational philosophy and data-flow system as described in detail on the Web (http://www.eso.org/org/dmd). The normal starting point in preparing proposals will probably be to consult the Instrument Description, Users Manual, etc. on the Web and to use the Exposure Time Calculators (ETC) referred to above to assess feasibility and estimate the required integration times. Proposals can then be submitted for either Service or Visitor Mode observations as described in ESO's Announcement for the relevant period. In both cases, the actual observations will be executed at the telescope via Observing Blocks consisting of acquisition and instrument (observation description) templates, which set the various, instrument functions and parameters and control the exposures via a sequencer. Real time feedback on the instrument status and the progress of the observations is provided via the Observing Software display on the instrument workstation and the actual images are displayed on a Real Time Display (RTD). The RTD is also used interactively in some modes e.g. to 'drag' objects seen in the imaging mode into the slit for spectroscopy and to determine pixel values, coordinates, image quality, etc. All raw data are archived as are those reduced by the reduction pipelines whose current status is described separately by Devillard et al. in this issue. Additional observations defined in a Calibration Plan will also be conducted by ESO in order to maintain the instrument performance, analyse trends (e.g. in zero point, dark and flat field variations) and to allow calibration of Service Mode data to a specified level.

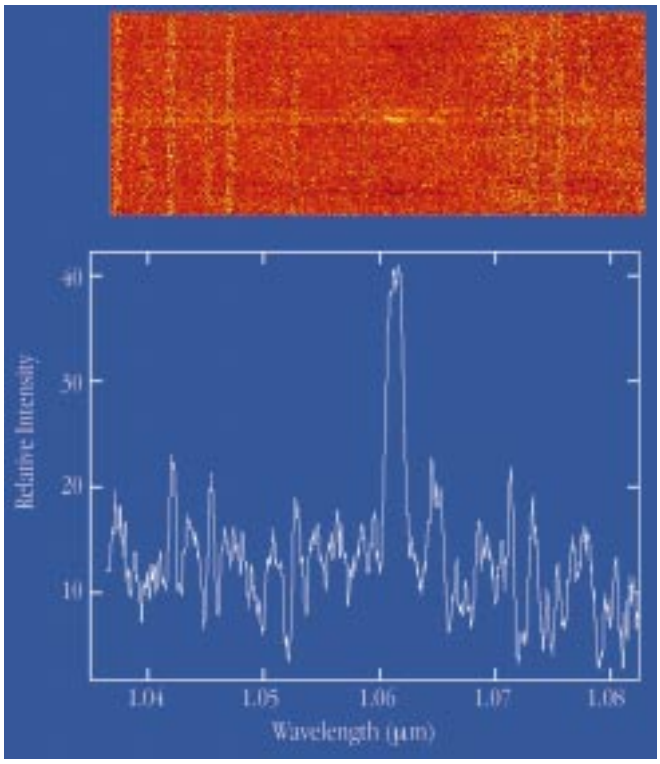

Figure 7: The upper panel shows a medium resolution (R ~ 3000) spectral image around 1.06 μm of two galaxies at z ~ 0.62 selected from the CFRS catalogue. Total exposure time was 1 hour. The lower panel shows the extracted spectrum of the brighter galaxy which, in addition to the continuum, shows bright redshifted Hα and fainter [NII] (to the right) emission lines. As can be seen in the image, the Hα emission appears to be tilted relative to the continuum due to the rotation of the galaxy which can thus be measured to provide an estimate of its mass.

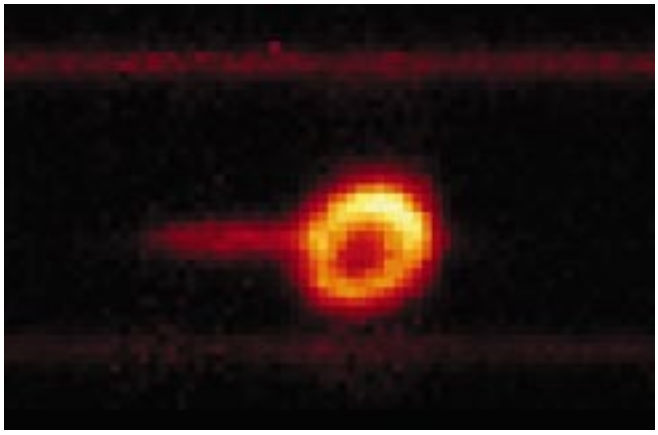

Figure 8: A spectral image of SN 1987A in the HeI (1.083 μm) line obtained in a 20-min exposure using the medium-resolution grating and a 2″ wide slit. The ring is formed of gas blown off the progenitor star during its evolution and which was first photoionised by UV light from the SN and more recently shock ionised by ejecta which, travelling at 30,000 km/s, has only just reached it after a travel time of nearly 12 years. The jet-like feature extending to the left is actually in the spectral dispersion direction and shows the presence of a blue-shifted, high-velocity component that is believed to arise in the ionised ejecta.

7. Acknowledgements

We wish to particularly thank the ISAAC Science Team R. Chini, G. Miley, E. Oliva and J.-L. Puget for their suggestions and encouragement throughout the design and development phase; R. Gilmozzi, P. Gray, M. Petr, G. Rahmer and P. Sansgasset for their support during installation and commissioning on Paranal and J. Alves, P. Amico and M. Kissler-Patig in Garching. Collective thanks are also due to many other people, too numerous to mention individually and within all Divisions of ESO, who have contributed to this project. We are also grateful to L. Tresse and O. Le Fèvre for detailed information on the CFRS galaxy sample.

References

Hammer, F., Crampton, D., Le Fèvre, O., Lilly, S.J. 1995, *ApJ*, **455**,88.

Lizon, J.-L. 1996, *The Messenger*, **86**, 11.

Meyer, M., Finger, G., Mehrgan, H., Stegmeier, J., Moorwood, A.F.M.: 1996, *The Messenger*, **86**, 14.

Moorwood, A.F.M. 1996, In Optical Telescopes of Today and Tomorrow (ed. A. Ardeberg), *SPIE* Vol. 2871, 1146.

amoor@eso.org

ISAAC Pipeline Data Reduction

N. DEVILLARD, Y. JUNG, J.-G. CUBY, ESO

The ISAAC pipeline, just as the pipeline for any other VLT instrument, is built to provide reduced data on site in order to assess their quality as soon as possible. Another version of the same software will also be running in Garching for quality control, trend analysis, and service-observing data-reduction purposes. All instrument pipelines share the same generic structure, taking care of data handling, i.e. transfers and reduction recipe triggering. The recipes themselves are specific to each instrument, they are plug-ins hooked into this generic data-handling structure, and they can be described as specialised tasks attached to an instrument-acquisition template. For more details about pipelines and Data Flow, the reader is referred to the ESO Web pages and corresponding reference documents.

The following instrumental modes are supported in pipeline mode for the first ISAAC period: imaging jitter, twilight flat, darks and bad pixel map creation, illumination frames and zero-point computations. In spectroscopy: NodOnSlit, flat-field, spectroscopic response function, star trace calibration, and slit position. We give here an overview of the algorithms used to reduce the data without user intervention for all these modes, so that observers can get a rough idea of what is done in pipeline mode, what the working domain for the recipes is, what can be obtained in the control-room at runtime, and how to reproduce these reduction processes at their home institute if they wish to.

1. Imaging Mode

Imaging recipes (procedures) are based on the ESO **eclipse** library, mainly to speed up the number-crunching process (see article in *The Messenger* No. 87, p. 19–20). The eclipse library is exportable, compiles on virtually any (recent) Unix machine that has minimum POSIX compatibility, and is available on the Web at the following address: http://www.eso.org/eclipse/

Calibration recipes

Dark frames are acquired through a dedicated template, which stores several dark frames for each possible DIT (Detector Integration Time), and usually